Energy Conversion and Management: X 13 (2022) 100158

Contents lists available at ScienceDirect

Energy Conversion and Management: X

journal homepage: www.sciencedirect.com/journal/energy-conversion-and-management-x

Towards solvothermal upcycling of mixed plastic wastes: Depolymerization pathways of waste plastics in sub- and supercritical toluene

Nepu Saha, Soudeh Banivaheb, M. Toufiq Reza *

Department of Biomedical and Chemical Engineering and Sciences, Florida Institute of Technology, 150 West University Boulevard, Melbourne, FL 32901, USA

ARTICLE INFO

Keywords:
Solvothermal liquefaction
Polypropylene
Polystyrene
Polyurethane
Plastic wastes
Sub-and supercritical toluene

ABSTRACT

Solvothermal liquefaction (STL) is a thermochemical conversion process, where a waste feedstock is treated with sub-and supercritical solvents. The key objective of the study was to investigate how a one-step STL using toluene as a solvent can degrade hard-to-recycle waste plastics (#5–#7). Three different plastic wastes namely, polypropylene (#5), polystyrene (#6), and polyurethane (#7), and their equal mixture (by weight, also referred here as mixed plastic wastes) were solvothermally liquefied by toluene in a 7 mL pressure bomb at 300, 350, and 400 °C for 3, 6, and 9 h in order to determine the effect of temperature and time, respectively. The liquid products were separated from the solid residue and further analyzed in terms of the STL conversion, change in elemental compositions via ultimate analysis, boiling point distribution via thermogravimetric analyzer (TGA), alteration of chemical bonds via proton nuclear magnetic resonance spectroscopy (^{1}H NMR), and degradation products via gas chromatography mass spectroscopy (GCMS). The results showed that the STL conversion increase with the increase of reaction temperature and time. From the elemental analysis, it can be predicted that the higher heating values of the crude products are between 30 and 45 MJ/kg. Boiling point distribution showed that the production of lower hydrocarbon (C_8–C_{20}) increased significantly from about 10% at 300 °C to 80% at 400 °C. Additionally, product distribution showed that the aromaticity increased with the increase of residence time where the main products are benzene and styrene like products. Overall, it was observed that mixed plastic wastes have a synergistic effect on the degradation products.

1. Introduction

In the United States, about 35.7 million tons of plastic wastes were produced in 2018, which was 12% of the total municipal solid waste generated in the same year [1]. Most of the plastics are single-use, therefore, only 8.7% of the plastic waste was recycled and the rest were incinerated or landfilled. The recyclability of plastics depends on the type of plastics. For instance, polyethylene terephthalate (PET, #01) and high-density polyethylene (HDPE, #2) are relatively easier to recycle at the material recovery facility (MRF). However, polyvinyl chloride (PVC, #03), low-density polyethylene (LDPE, #04), polypropylene (PP, #05), polystyrene (PS, #06), and polyurethane (PU), polycarbonate, BPA, and other plastics (#07), respectively, are relatively difficult to recycle economically. Moreover, #05–#07 are often contaminated with organic and inorganic impurities and also have low bulk density. As a result, most of these #05–07 plastic wastes are either landfilled or incinerated [2].

While plastic wastes possess a serious environmental liability, on the other hand, #05–07 plastic wastes are negative-value feedstocks with huge potential to be upcycled to high-value liquid fuel and chemicals. There are various techniques emerging for converting solid wastes to valuable products, such as pyrolysis, gasification, and hydrothermal liquefaction (HTL). Pyrolysis of plastics produces energy-dense crude oil and gases [3–5], however, due to certain limitations (e.g., separation of non-plastic), this process is often restricted to prevent potential dioxins formation [6–8]. On the other hand, gasification of plastics can be used to produce syngas [9], which can then be used to make fuels or chemicals, however, it can destroy C–C bonds [10]. In addition, pyrolysis and gasification can significantly emit toxic gases, such as CO, dioxins, etc. [11–13]. When it comes to the degradation of organic wet wastes (e.g., sewage sludge, municipal solid wastes, animal manures), sub-and supercritical water are excellent choices as the feedstock does not need to be dried and water is a safe solvent [14–17]. The process, often called HTL, has been applied for upgrading more than hundreds of waste feedstocks. However, plastics turned out to be less reactive with water compared to the other organic wasted feedstocks (e.g., food waste, plant

* Corresponding author.
E-mail address: treza@fit.edu (M. Toufiq Reza).

https://doi.org/10.1016/j.ecmx.2021.100158
Received 11 October 2021; Received in revised form 3 December 2021; Accepted 5 December 2021
Available online 9 December 2021

waste, etc.) [18–19]. Also, HTL defeats the purpose as plastic wastes are often dry and have minimal oxygen content. Introducing water as solvent, a significant amount of carbon is usually lost in the aqueous phase (HTL wastewater) and more oxygenated products are formed, which require expensive separation and hydrodeoxygenation steps. For instance, Seshasayee and Savage [14] found that HTL of PP, PS, and polycarbonate under near-and supercritical water significantly increases the O/C ratio of the product oil while no oxygen was present in the raw PP and PS feedstocks.

In addition to water, other organic solvents have been used for liquefaction including methanol, ethanol, propanol, and acetone [20,21]. This process is known as solvothermal liquefaction (STL). There are two major advantages of STL, namely (i) organic solvents generally have low critical temperatures and critical pressures, resulting in reactions at lower operating conditions, and (ii) solvent regeneration and resue are less energy-intensive. However, using oxygenated solvents add risks of oxygen contamination of the finished products and also add cost to the process that requires either separation or a market that can accommodate an oxygenated crude as oil/solvent. In fact, in the cases of alcohols used for STL, the oxygen content of the solvent was reported to be undesirable for many fuel-based purposes [20,22–24]. An exception to these oxygenated solvents, a non-oxygenated solvent (i.e., toluene) can be used to deconstruct the plastic wastes. Toluene is a nonpolar solvent with low critical temperature and critical pressure compared to water (toluene: critical temperature = 318 °C and critical pressure = 598 psi; water: critical temperature = 374 °C and critical pressure = 3200 psi). Nonpolar degradation products are likely to readily dissolve in toluene, which will result in ease of product separation. Although there is a wealth of literature on toluene assisted separations of hydrocarbons [25–27], to the best of the authors' knowledge, no such study has been conducted to explore STL phenomena of plastic wastes in presence of toluene.

Therefore, the aim of this study was to answer some of the critical questions about the STL of #05–#07 plastic wastes using toluene as solvent under sub-and supercritical temperatures. The research questions of the study are: (1) what are the reaction mechanisms of STL for individual plastics? (2) how the product formation changes with reaction severity? (3) plastics are likely to be mixed, therefore, how mixed plastics perform STL compared to their theoretical blend? To answer these questions, three plastic precursors (PP, PS, and PU), including a mixture of them (in equal weight ratio) were used as feedstocks while toluene was used as a solvent for STL. All the STL experiments were conducted at a temperature between 300 and 400 °C for a residence time between 3 and 9 h. In order to investigate the product characteristics, ultimate analysis was conducted for the prediction of the higher heating value of the crude product, product distribution was determined for the thermogravimetric analysis (TGA). To further confirm the product distribution, crude products were analyzed in gas chromatography mass spectrometry (GCMS). Furthermore, proton nuclear magnetic resonance (^{1}H NMR) was conducted to investigate the change in chemical bonds of the products.

2. Materials and methods

2.1. Materials

In this study, Fisherbrand polypropylene (PP) centrifuge tube was used as the source of #5 plastic, while the polystyrene (PS) tube holder of the centrifuge tube was used as the source of #6 plastic. Both of these materials were purchased from Fisher Scientific (Waltham, MA). On the other hand, a commercial polyurethane (PU) mattress was used as the source of #7 plastic. All of these three precursors were added in the same weight ratio (1/3 of each) for making the mixed (MIX) plastic feedstock. The elemental analysis and the particle size of the raw plastics are shown in Table 1. The solvent, toluene (American Chemical Society (ACS) reagent grade), used in this study was purchased from Fisher Scientific (Waltham, MA).

Table 1
Elemental analysis and particle size of the raw plastics.

Feedstock	Elemental analysis (wt%)				Particle size (mm)	
	C	H	N	O + ash	Length	Width
PP	83.14	13.06	BD*	3.86	3.64 ± 0.66	2.18 ± 0.30
PS	88.5	8.18	BD*	3.3	4.54 ± 0.94	3.12 ± 0.47
PU	69.05	9.28	5.75	15.93	4.36 ± 0.41	3.52 ± 0.86

*BD: Below detection limit.

2.2. Experimental methods

Custom-made stainless steel (SS-316) reactor vessels (volume 7 mL) were used to perform STL experiments. The experiments were performed at 300, 350, and 400 °C to cover subcritical and supercritical regions of toluene. In a typical STL experiment, 1:10 (wt/wt) dry feedstock to toluene was fed into the reactor. The loading (0.48 g precursor and 4.77 g toluene) was chosen to minimize the headspace in the reactor; so that, the reaction could reach at the supercritical state while the temperature of the experiment was more than the supercritical temperature of toluene. The reactor was heated using a preheated Techne SBL-2 sand bath (Vernon Hills, IL) at one of the set temperatures of 300, 350, or 400 °C. The reactor was submerged into the sand bath throughout the residence time of 3, 6, or 9 h. As soon as the residence time was over, the reactor was taken out from the sand bath and let it cool by natural convection. When the reactor reached at room temperature, it was opened and the content was filtered through a 1 μm glass fiber syringe filter purchased from Tisch Scientific (North Bend, OH). After filtration, the syringe filter was dried in the oven at 105 °C for 24 h to determine the solid mass yield. The remaining mass was considered as the STL conversion. This mass could be responsible for both gaseous and liquid products. Since each of the experiments was conducted in batch operation mode and the gaseous products vented to the atmosphere, only the liquid products were considered for further analysis. The filtered liquid crudes were collected in glass vials and stored in a refrigerator until further characterization. The STL crudes are named as F-T-t, where F stands for feedstock (e.g, PP, PS, PU, MIX), T stands for STL temperature in °C, t stands STL residence time in h. All the STL experiments were triplicated in order to check the reproducibility of the experiments.

2.3. Crude product characterization

Elemental analysis of the STL crude products was carried out in a Thermo Scientific Flash 1112 Organic Elemental Analyzer (Waltham, MA). Since the crude was dissolved in toluene, a certain amount of (about 20 μl) the mixture was first dried (remove the toluene) on an aluminum sample pan (designated for elemental analyzer) by natural convection. While the excess toluene dried off from the crude product, the dry sample was prepared with other standards. For the CHNS analysis, 2,5-Bis (5-*tert*-butyl-benzoxazol-2-yl) thiophene (BBOT) was used as a calibration standard and vanadium oxide (V_2O_5) as a conditioner for the samples, which were combusted around 950 °C in ultra-high purity oxygen with a helium carrier gas and passed over copper oxide pellets and then electrolytic copper. The gases were then analyzed by a thermal conductivity detector (TCD), with the peak areas of detection being compared to that of BBOT standards. Oxygen and ash contents were calculated by the difference method.

The higher heating value (HHV) of the STL crude was estimated with the modified Dulong formula proposed by Hosokai *et al* [28]:

$$HHV\left(\frac{MJ}{kg}\right) = 0.3383C + 1.422\left(H - \frac{O + ash}{8}\right)$$

where C and H are the wt.% of carbon and hydrogen, respectively, determined from the elemental analysis. Although, the original Dulong equation use only O which is the representation of elemental oxygen, O plus ash was use instead as we did not measure the oxygen and ash separately. Please note that the HHV is not reported as ash-free, as we have included oxygen and ash together.

The boiling point (BP) distribution of the hydrocarbons in the STL crude products was determined by using a Q5000 thermogravimetric analyzer (TGA) (TA Instruments, New Castle, DE). The experiments were carried out under the inert atmosphere using a constant nitrogen flow (10 mL/min). The heating rate was maintained at 20 °C/min throughout the experiment. The samples were first heated from 25 to 115 °C and kept isothermal for 5 min to make sure no excess toluene remained in the samples. The temperature was then increased from 115 to 600 °C following by cooling down to the room temperature. Based on the boiling points of various hydrocarbons, a product distribution was calculated from the thermogram. For instance, the TGA curve of each product summarises the weight loss within different temperature ranges. The weight loss within a specific boiling point range is considered the percentage of corresponding hydrocarbons. A similar methodology was previously used in a study conducted by Seshasayee and Savage [14]. A schematic of this calculation is shown in the Supplementary information (SI) document (see Fig. S1).

The crude oil was analyzed with ^{1}H NMR to identify the presence of aliphatic and aromatic hydrocarbons in it. The ^{1}H NMR of the crude oils was determined in a 400 UltraShield^{TM} Bruker NMR spectrometer (Billerica, MA) operating at a resonance frequency of 300 MHz and accumulating 16 scans. The spectra were recorded from 0 to 10 ppm. STL crudes were dissolved in toluene with a 1:9 crude to solvent ratio. As the STL crude was dissolved in toluene, an additional deuterated solvent (Benzene-d_6) in a capillary was inserted in the NMR analysis tube to minimize the solvent peak intensity. According to the literature, toluene showed two distinct peaks at 2.3 ppm and 7.0–7.3 ppm [29–31]. So, for further analysis of the result, we have ignored those two peaks as STL product peaks.

Gas chromatography was performed on the samples using gas chromatography mass spectrometry (Agilent 7890 GC combined with a 5975 Mass Spectrometric Detector). The GC was equipped with an Equity 1701 (Supelco) column (60 m × 0.25 mm, 0.25 μm). The inlet was held at 250 °C with a split ratio of 1:1 and helium flow of 5 mL/min. The oven was held at 45 °C for four minutes, increased to 280 °C at a rate of 3 °C/min, and finally held at 280 °C for 20 min. An internal standard (n-decane, 99%, MilliporeSigma) with no overlapping chromatogram peaks was doped (0.1 wt%) into all samples prior to injection. Compound identification was further performed by using the NIST mass spectral database.

3. Results and discussion

3.1. Degree of depolymerization with the increase of STL reaction severity

The solid yields and STL conversion from the different plastics, as well as the MIX, are shown in Fig. 1. In general, the STL conversion increases with the increase of both reaction temperature and retention time, while the solid yield decreases with the increase of reaction time and temperature (except for the PS). The PS showed that all the samples that went to the conversion (gas and/or liquid) phase are either reacted or dissolved in the solvent. A similar observation was reported by Seshasayee and Savage [14], where PS derived crude (oil) production was significantly higher compared to the PP derived crude. However, the STL conversions for the PP samples at 300 and 350 were significantly low (5–11% and 16–36%, respectively), whereas it is increased to 100% at 400 °C and 9 h and the rate of change was the maximum between 3 h and 6 h. Similar observations were reported earlier but with water as solvent. Sub- and supercritical water assisted the plastic degradation with acid- and base-catalyzed reactions which expedited the depolymerization process [32]. Another study reported that the plastic (PS) degradation was further enhanced with the increase of supercritical temperature of the solvent and moved to gaseous products from the liquid composition [33]. Despite of no oxygenated compound presented for the PP and PS feedstocks, this study shows high crude production, which indicates depolymerization of PP and PS with supercritical toluene. The reason for higher conversion at 400 °C could be due to the excessive depolymerization reactions breaking down the solid

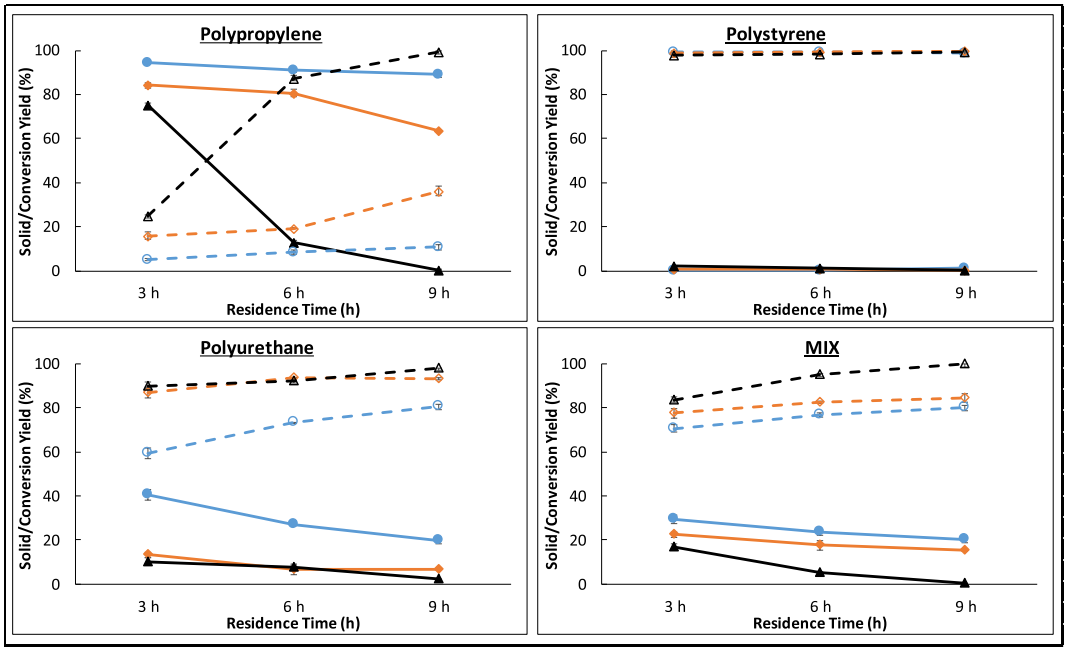

Fig. 1. Yields at various reaction temperatures and residence times. Solid lines represent the solid yields while dotted lines indicate the STL conversion yields. Reaction temperatures are denoted with the color codes of the lines where blue, orange, and black lines indicate the temperature of 300, 350, and 400 °C, respectively. (For interpretation of the references to color in this figure legend, the reader is referred to the web version of this article.) (For interpretation of the references to color in this figure legend, the reader is referred to the web version of this article.)

component into smaller crude phase molecules [32]. Furthermore, the higher conversion of PS compared to the PP could be due to having the lowest dissociation energy of the benzylic C–C bond in PS (333 kJ/mol) compared to the other polyolefin bond (356 kJ/mol) examined in the PP [34]. The conversion of the PU increased with the increase of temperature from 300 to 350 °C, however, with further increase of the temperature to 400 °C did not show any further change in the conversion. This could be because in both cases (at 350 and 400 °C) the solvent was at the supercritical condition and oxygen was present in the reaction medium, which resulted in depolymerization reaction along with the deoxygenation, dehydration, and decarboxylation reaction [14]. Although the yield did not change significantly, the products could be different in those cases. To identify the product distribution, further characterizations were conducted and discussed in the following sections. Similar to the individual precursor, the STL conversion increased for MIX feedstock with the increase of reaction temperature and residence time. It was observed that the MIX had higher experimental STL conversion than the theoretically calculated conversion (see Fig. S2). This could be due to the synergistic effect during the plastics depolymerization. The theoretical conversions were calculated by multiplying the conversions with the one-third (as each precursor was added equally in the experiment). The presence of oxygen and nitrogen in the PU precursor could enhance the depolymerization of the PP via decarboxylation and/or denitrification reactions, ultimately increased the conversion. The STL products were further investigated in terms of liquid crude.

To see how various STL conditions affect the elemental composition of the crudes and their corresponding heating value, elemental analysis were conducted. Fig. 2A shows the elemental analysis of the STL crudes derived from MIX. The rest of the elemental analyses of the individual waste plastics are shown in Table S1. It can be noted that the at subcritical condition, residence time play an import role in degrading MIX as Fig. 2A indicates that the carbon content varied between 64 and 79% with the residence time between 3 and 9 h. On the contrary, the O content reduced from 25 to 8% with the increase of residence time. For instance, at 3 h, the C content was similar to the raw sample (about 79%). However, with the increase of residence time to 6 h, it was observed the C content decreased to 64% while the O content increased to 25%. This could be due to the time dependence of the PU degradation under subcritical conditions discussed in the earlier section. With further increase of residence time (from 6 to 9 h), the C content went up which indicated that over the longer period of reaction, deoxygenation reaction could propagate that reduces the O content in the crude product. On the other hand, at supercritical conditions (350 and 400 °C), no significant change in the elemental composition was observed with the increase of residence time. This might be due to at supercritical conditions, MIX might have very fast reaction kinetics. The line graph in Fig. 2B represents the estimated HHV from the elemental compositions. It indicates that the estimated HHV of the mixed plastic wastes derived crude is about 30–37 MJ/kg. However, the predicted HHV of some of the PP derived crudes (e.g., PP-360–3/6/9) are about 45 MJ/kg. These values are comparable to the HHV of raw petroleum crudes (40–45 MJ/kg) [14]. The estimated HHV of each precursor including mixed plastic (theoretically calculated) were well above compared to their corresponding crudes, however, the product distribution (targeted lower hydrocarbons) of the crudes could further elucidate the chemical structure of the depolymerized products.

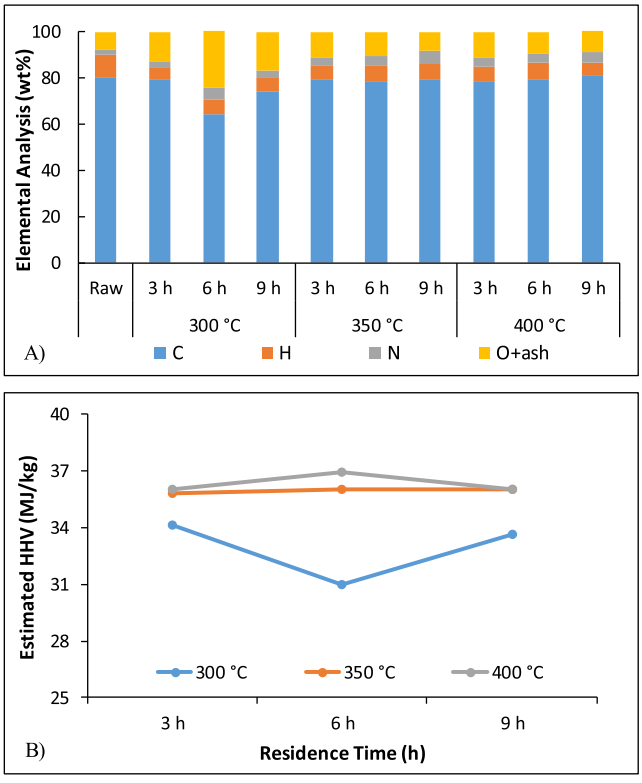

Fig. 2. A) Elemental analysis of crudes derived from mixed plastic wastes. B) The estimated higher heating value of the corresponding crudes.

3.2. Boiling point distribution of the crude

As the main focus of this study was to propose a depolymerization mechanism of various plastic wastes, the crude products were further investigated in terms of their boiling point (BP) distribution. The BP distributions of the crude products are shown in Fig. 3. The BP distributions of the crude products were divided in terms of four different hydrocarbon cuts, such as $< C_8$ (BP < 125 °C), C_8–C_{20} (BP in between 125 and 340 °C), C_{20}–C_{50} (BP in between 340 and 560 °C), and $> C_{50}$ (BP > 560 °C) [35]. The crude produced from the PP showed that at 300 °C, the PP just dissolved in the solvent resulted in a similar distribution compared to the raw PP. The effect of the residence time at 300 °C was not significant. At 350 °C, about 10% of C_8–C_{20} product was observed where most of the products were still in the C_{20}–C_{50} region. However, a major change was observed at 400 °C, where the higher hydrocarbons are broken into lower hydrocarbons at higher residence time (6 and 9 h). For instance, about 90% of the produced crude were in the C_8–C_{20} region including about 5% even lower than C_8. From this observation, it can be hypothesized that the PP first dissolved into the solvent, then depolymerized, and the longer residence times enhance the depolymerization to produce lower hydrocarbons. Similar to the PP; PS and PU showed that most of the products with the C_{20}–C_{50} region at 300 °C. However, an impact on the distribution was observed from the 350 °C, where about 50% of the products were in the C_8—C_{20} region. At 400 °C, the PS and PU behaved differently, where the PS degraded mostly (around 95%) into C_8–C_{20} hydrocarbons. On the other hand, some of the PU remains undegraded even at the highest residence time (9 h). In addition, some new repolymerized products ($>C_{50}$) were produced which could be due to the agglomeration reactions of the lower hydrocarbons. The mixed feedstock followed a similar trend of the individual precursors where the most significant effect on the BP distribution occurred at 400 °C. Similar to the crude yield results, the BP distribution also confirmed the synergistic effect of the mixed feedstock. Wherein some of the cases up to 20% higher C_8–C_{20} products were observed experimentally compared to the theoretically calculated numbers. The theoretically calculated BP distribution is shown in the SI document (see Fig. S3). From Fig. 3 and Fig. S3, we can see that both residence time and reaction temperature have an impact on the BP distribution. For a better understanding of the STL degradation, product identification was carried out in GCMS. Product identification was only carried out for 9 h experiments because they showed the highest crude yield and the distinct BP distribution among all residence time.

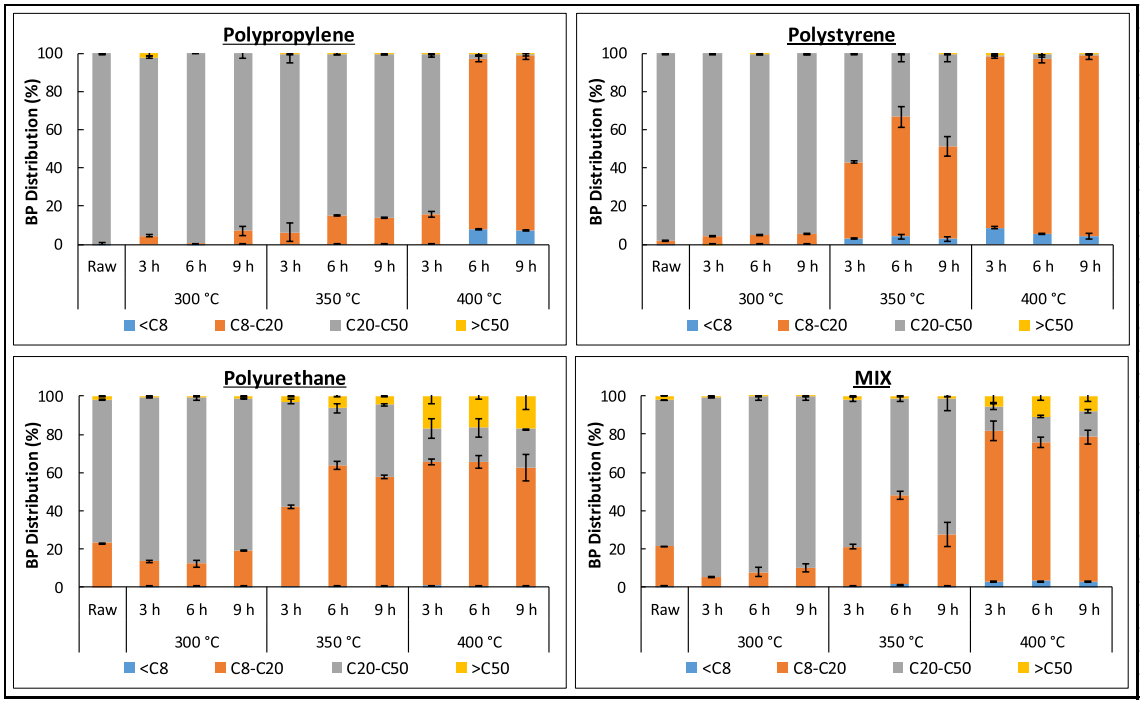

Fig. 3. BP distribution of the crude products at various reaction temperatures and residence times.

3.3. Product identification by GCMS

GCMS was the most preferred technique to identify the products in the synthesized crudes. Products obtained from different precursors were elaborated in Tables S1–S5, where a summary of major products and the product distribution are shown in Table 2 and Fig. 4, respectively. The reason behind not considering any compounds that appeared earlier than 12 min is that the crude was dissolved in toluene and the toluene peak in the GCMS comes around 12 min. In addition, it is noted that a certain percentage of the product was defined as beyond detection (BD) limit in Fig. 4. This BD indicates either the compounds were too big to detect within the runtime or they were not found in the library. From the chemicals identified in Fig. 4, there was no oxygenated and nitrogenated product in the PP and PS derived STL crudes which were expected as the PP and PS do not have nitrogen and oxygen in their structure. On the other hand, both PU and MIX crudes experienced oxygenated and nitrogenated products along with hydrocarbons. It can also be observed from Fig. 4 that these nitrogenated and oxygenated products are reduced significantly with the increase of residence time. In terms of hydrocarbons, generally, four groups of compounds are

Table 2
Major identified chemical compounds via GCMS in the STL crude produced from PS, PP, PU, and MIX treated at 400 °C for 9 h.

Feedstock	Compound	Formula	Retention time (min)	Peak area (%)		
				T = 300 °C	T = 350 °C	T = 400 °C
PP	Cyclohexane, 1,2,3-trimethyl-	C_9H_{18}	13.74	–	6.53	0.44
	Benzene, (2-methylpentyl)-	$C_{12}H_{18}$	33.22	–	33.16	0.40
	Bibenzyl	$C_{12}H_{18}$	49.97	15.68	2.47	3.67
	Benzene, 1,1′-(1,3-propanediyl)bis-	$C_{15}H_{16}$	59.21	–	–	16.88
PS	Ethylbenzene	C_8H_{10}	16.13	0.57	10.65	29.42
	Styrene	C_8H_8	17.97	14.67	40.95	7.22
	.alpha.-Methylstyrene	C_9H_{10}	22.23	0.68	5.70	1.38
	Bibenzyl	$C_{14}H_{14}$	50.11	2.89	10.32	11.46
	Benzene, 1,1′-(1,3-propanediyl)bis-	$C_{15}H_{16}$	57.99	51.85	9.38	20.24
PU	Ethylbenzene	C_8H_{10}	16.12	5.82	7.09	10.80
	Styrene	C_8H_8	18.01	12.30	1.52	0.21
	Benzene, propyl-	C_9H_{12}	20.43	–	1.95	8.31
	Benzene, butyl-	$C_{10}H_{14}$	25.93	3.53	16.71	21.20
	Benzenebutanenitrile	$C_{10}H_{11}N$	45.20	26.31	13.40	–
	Bibenzyl	$C_{14}H_{14}$	49.82	–	2.66	13.18
	1,3-Benzenediamine, 4-methyl-	$C_7H_{10}N_2$	50.40	15.83	–	–
	Benzene, 1,1′-(1,3-propanediyl)bis-	$C_{15}H_{16}$	56.22	22.57	36.70	8.64
MIX	Ethylbenzene	C_8H_{10}	15.98	1.30	4.17	10.32
	Styrene	C_8H_8	17.82	8.01	5.72	0.66
	Benzene, butyl-	$C_{10}H_{14}$	25.76	1.15	4.78	9.46
	Benzenebutanenitrile	$C_{10}H_{11}N$	45.21	6.56	–	–
	Diphenylmethane	$C_{13}H_{12}$	45.68	–	6.45	1.74
	1,3-Benzenediamine, 4-methyl-	$C_7H_{10}N_2$	52.41	40.32	–	–
	Benzene, 1,1′-(1,3-propanediyl)bis-	$C_{15}H_{16}$	61.58	28.17	60.80	28.86

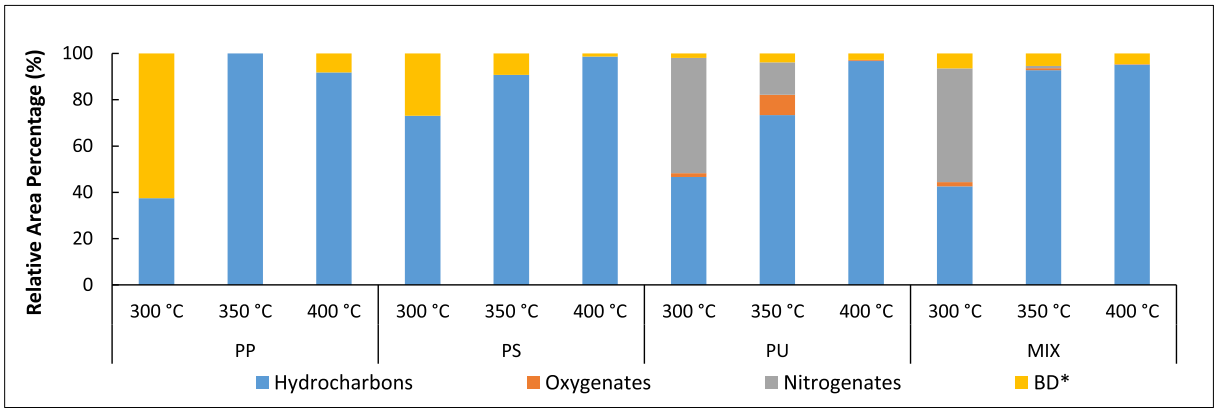

Fig. 4. The product distribution of GCMS functional compounds crudes produced at various reaction temperatures and 9 h residence time.

identified by GCMS analysis: aliphatic hydrocarbon (e.g., heptane), substituted cycloalkanes (e.g., cyclohexane), aromatic hydrocarbons (e.g., Benzene), and substituted polycyclic aromatic hydrocarbons for all samples. All the detected hydrocarbons in PP derived crudes are in the jet fuel range (C_8-C_{16}) shown in Table S2, which confirms the findings of the TGA. At 300 °C and 350 °C, the major components of the PP-derived STL crudes are aromatic; however, with increasing the temperature to 400 °C, in addition to increasing the variety of the product, the percentage of aliphatic light compound (cycloalkanes) increased, and it became the major products [36]. The product distribution of the PS derived crudes is shown in Table S3. It can be observed that, with increasing the time, the percentage of hydrocarbon is increased from 72.79% to 98.34%. As polystyrene has aromatic rings in its structure; therefore, it is expected that the STL crude is composed of a high fraction of stable aromatic compounds. The aromatic compounds formed were mostly benzene derivatives. At the lower temperature (300 °C), 1,3-diphenylpropane is the major product from STL crude from PS, which is likely formed by dimerization of styrene or ethylbenzene. However, upon raising the temperature to 350 °C, the 1,3-Diphenylpropane is decomposed to the lighter oil about 80%, mostly to styrene monomer, ethylbenzene, alpha-methyl styrene, and bibenzyl. It seems that higher temperatures cause diverse long-chain products and aromatic rings as the aromatics are stable in supercritical toluene. At PS-400–9, ethylbenzene was identified as the major product followed by styrene, which may subject the end chain scission degradation is a dominant pathway [37].

From the results in Table S4, it can be seen that about 50% of major products of MIX-300-9 are nitrogen compounds. With increasing the temperature from 300 to 400 °C, the percentage of this nitrogen compound (like 1,3-Benzenediamine, 4-methyl- and Benzenebutanenitrile) decreases considerably (about 42%) which shows that denitrification reaction mostly happens at the higher temperature. When the temperature increases to 350 °C, butyl-benzene ($C_{10}H_{14}$) and 1,1′-(1,3-propanediyl)bis- benzene ($C_{15}H_{16}$) are the major products, however with increasing temperature to 400 °C the 1,1′-(1,3-propanediyl)bis-benzene is broken to the lighter compounds like butyl- benzene, ethylbenzene, (2-methylpropyl)-benzene and 1-ethyl-3-methyl-benzene. Therefore, it shows that higher temperature not only helps to decrease denitrification and deoxygenation but also it helps to have lighter components.

From the GCMS results of MIX (Table S5), it can be seen and concluded that higher temperatures have an intensive effect on the reduction of nitrogen compounds. At 300 °C, about 50% of the major components (area percentage > 5%) is nitrogen compound; however, with increasing the temperature to 400 °C, there is no nitrogen compound remaining. Additionally, when the temperature is increased to 350 °C, the percentage of hydrocarbon is increased by about 54% which also has positive effects on the crude yield. The major product is 1,1′-(1,3-propanediyl) bis-benzene ($C_{15}H_{16}$) with an area percentage of 60%, which is then degraded with increasing the temperature to 400 °C to lower hydrocarbons like butylbenzene, ethylbenzene, and lighter aliphatic compounds (cycloalkanes). The GCMS results are complementary to the BP distribution of crude products, as a higher percentage of lighter hydrocarbons formed at 400 °C and 350 °C for 9 h compared to 300 °C.

3.4. Proposed reaction mechanism of STL

To understand the degradation mechanism of the studied plastics, the crude products were further analyzed using ^{1}H NMR and the findings were compared with the GCMS results and a possible reaction mechanism is proposed. The ^{1}H NMR spectra of STL crude products at 9 h residence time are shown in Figs. S4–S6. As the products were dissolved on toluene, the most significant peaks were found at 2.3 and 7.0–7.3 ppm, which were expected as per literature [29–31]. Those peaks were such dominated that other peaks were not visible in the diagram. As a result, the spectra were zoomed in to see the different functional groups and explained in Fig. 5. The spectra of the crude products showed peaks at 0–1.5 ppm indicating aliphatic functional groups. With the increase of the STL temperature, the intensity of those groups increased for each studied feedstock. The peaks at 1.5–3.0 ppm indicate the presence of heteroatomic or/and allylic and alkyl compounds in the crude products. As there was no heteroatom presence on the PP and PS feedstock, those peaks should mostly be allylic alkyl compounds unless the feedstock had trace amount heteroatoms contamination. The peaks between 3.0 and 4.4 ppm represent the protons of alcohols, ethers, and esters, where 4.4–6.0 ppm indicate the methoxys and carbohydrates. The key finding from the NMR is that the supercritical toluene could degrade the longer chain plastic into short-chain monomer, aliphatic, and aromatic compounds. These molecules could be further degraded (reduced) with the increase of supercritical toluene temperature as well as the residence time.

In the case of PP, about 60% of detected hydrocarbons were aromatic compounds at PP-300–9, which increased with the increase of temperature (see Fig. S7). Although the PP is a long-chain polymer, the product crude contains a significant amount of aromatic mostly benzene related products which could be due to either chain end scission of the long aliphatic chain to make the gaseous product (e.g., CH_4) and shorter chain hydrocarbons following by the cyclization and aromatization reaction to form aromatic hydrocarbons or the shorter chain hydrocarbons polymerized and formed aliphatic products. For instance, at 400 °C, cyclohexenes could be formed by intramolecular cyclization of alkyl radicals or by radical addition reactions which could further undergo aromatization followed by addition reactions to form the alkyl-substituted naphthalene observed in GCMS analysis (section 3.3). At the same time, On the other hand, no aliphatic compound was observed within the detected compounds from PS derived crudes which could be

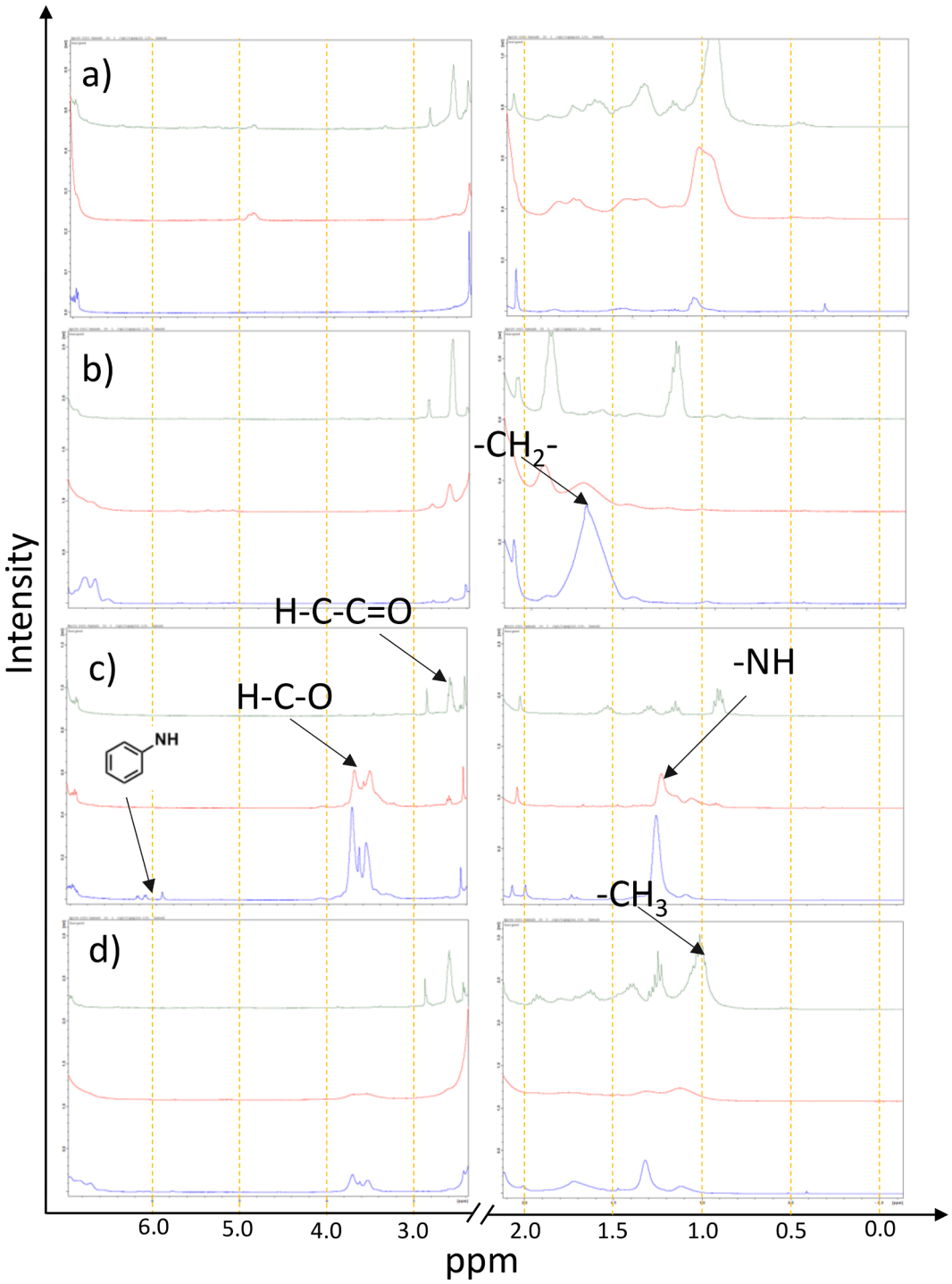

Fig. 5. ^{1}H NMR spectrum of plastic wastes while they were treated at various reaction temperatures and 9 h residence time where a, b, c, and d indicate PP, PS, PU, and MIX, respectively. Note that, the green, red, and blue color lines are for 400, 350, and 300 °C, respectively. (For interpretation of the references to color in this figure legend, the reader is referred to the web version of this article.) (For interpretation of the references to color in this figure legend, the reader is referred to the web version of this article.)

due to the presence of an aromatic ring in the feedstock. From the product distribution (Table S3), it can be speculated that the C–C bond either between two styrene molecules or the methyl groups broke first and formed the benzene/styrene, short alkyl chain, and gaseous product (e.g., CH_4) following by the polymerization reaction of the styrene/benzene molecules with aliphatic ends. The presence of aliphatic ends has already been confirmed from the ^{1}H NMR analysis earlier.

The degradation mechanism of PU could be different than PP and PS, as PU is a complex compound consisting of carbon, hydrogen, nitrogen, and oxygen. From the GCMS data and ^{1}H NMR results, it could be hypothesized that the PU undergoes various reactions (e.g., deoxygenation, decarboxylation, denitrification, polymerization, etc.) during the STL treatment. First, the PU degrade into shorter polymers. The short polymers could simultaneously form urethane monomers along with non-reacted isocyanate compounds. The monomer could finally deoxygenate, decarboxylated, denitrified, and form CO_2, NO_2 which remained

soluble in the liquid phase under high experimental pressure (saturation pressure of toluene > 40 bar). In addition, the monomer could degrade into other compounds, such as olefin ethers. With the higher residence time, these compounds could be added with the aromatic rings and from the oxygenated and nitrogenated compounds. GCMS results further confirm that the percentage of longer chain of hydrocarbons is increased, which could be due to polymerization reactions promoted by longer reaction time and temperature [38]. The MIX feedstock should follow the degradation mechanism of individual substrates, however, they or their monomers or degraded products could interact themselves and form new products. From the earlier findings, it was also observed that PS and PU degraded faster than PP. In the case of MIX plastic, the degradation of PS and PU could form intermediate solvents, such as 2-(1-methylethoxy)-1-Propanol (see Tables S3 and S4) which further enhanced the PP depolymerization. In addition, degradation of PU in the MIX feedstock could form intermediate solvents (see Table S4) which further enhanced the PP depolymerization. Due to these phenomena (which is defined as the synergistic effect in the earlier section), the product distribution in the MIX feedstock was a little different than the theoretically expected distribution. As for all of the feedstocks, a common finding was observed that with the increase of residence time production of aromatic products increased which indicated that the breakdown of aromatic ring was less likely while there is a possibility to form aromatic compound during the STL treatment. Based on the above discussion, a degradation mechanism of the plastic waste under sub and supercritical conditions of toluene has been proposed and shown in Fig. 6.

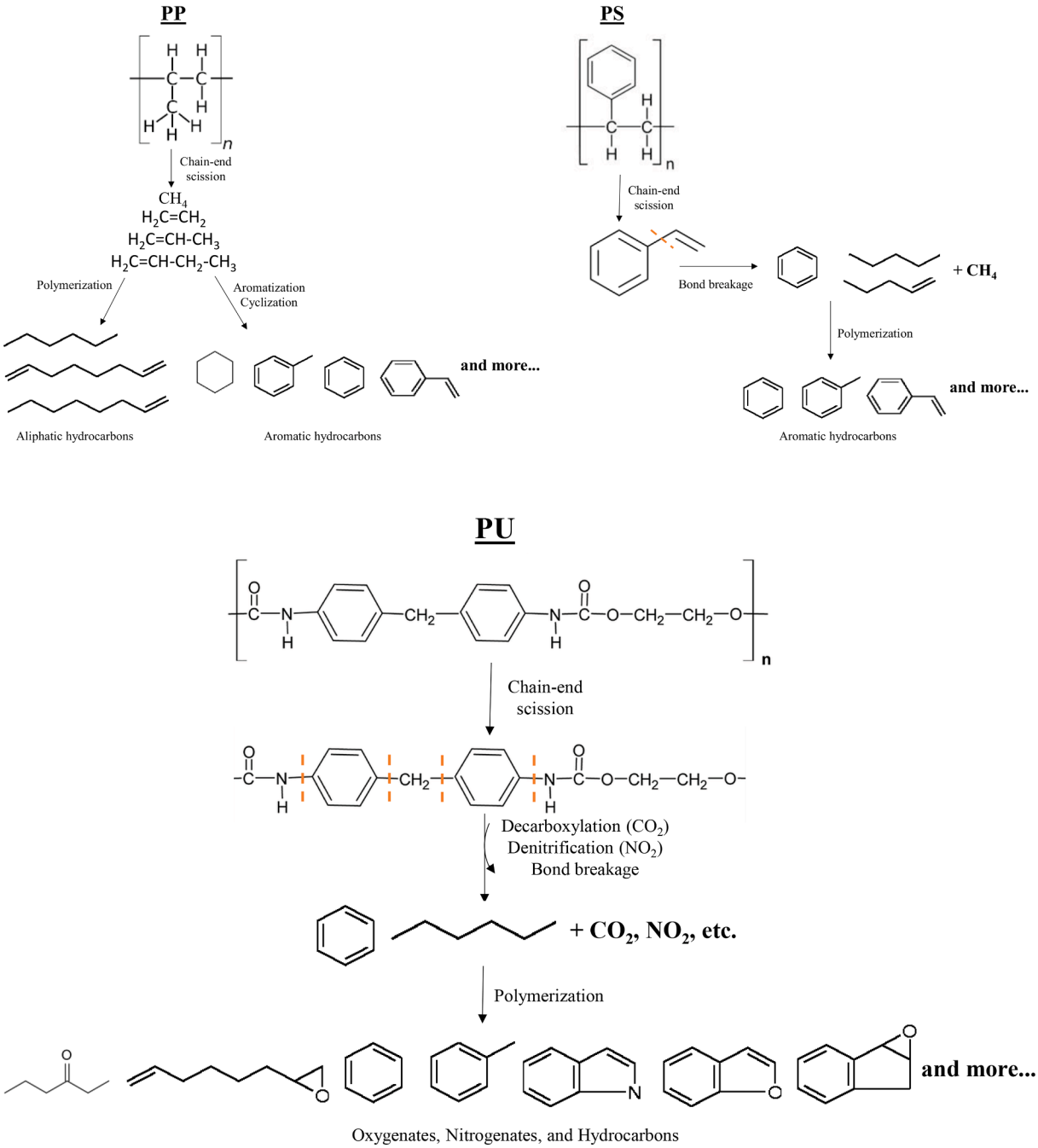

Fig. 6. Proposed degradation mechanism of PP, PS, and PU under sub and supercritical environment of toluene.

4. Conclusions

In conclusion, waste plastics (#5–#7) are depolymerized into crude products under sub and supercritical toluene. Both reaction temperature and residence time showed a positive impact on the STL conversion, although supercritical toluene has proven to be more effective on the depolymerization of hard-to-break polymers like PP. Production of lower hydrocarbon (C_8–C_{20}) increased significantly with the reaction severity. This study confirms that the mixed plastic showed a synergistic effect under STL conditions. In terms of reaction mechanism, PP experiences chain breakage followed by cyclization and aromatization, where PS is encountered with the impairment of the C–C bond followed by the polymerization reaction of the styrene molecules. On the other hand, PU undergoes decarboxylation, denitrification, bond breakage, and polymerization reactions. This study only focused on the liquid product from STL conversion; however, the gaseous products could also be a significant part of this treatment. So, in the future, a detailed analysis of gas and liquid products along with the remaining solid could add more value to the research community.

CRediT authorship contribution statement

Nepu Saha: Conceptualization, Data Curation, Formal Analysis, Writing-orginial draft, Writing-review and editing. **Soudeh Banivaheb:** Data Curation, Formal Analysis. **M. Toufiq Reza:** Funding acquisition, Conceptulatization, Writing-review and editing, Project administration.

Declaration of Competing Interest

The authors declare that they have no known competing financial interests or personal relationships that could have appeared to influence the work reported in this paper.

Acknowledgment

The research is partially funded by the National Science Foundation grant (1856058). The authors acknowledge Dr. Andrew Wagner from Mainstream Engineering Corporation for his assistance with GCMS. Special thanks to Dr. Mariefel Olarte, Dr. Michael Thorson, and Mr. Andrew Schmidt from Pacific Northwest National Laboratory for meaning discussions on solvothermal liquefaction. The authors would also like to acknowledge Md Tahmid Islam, Thomas Quaid, Aaron Portell, and Laura Guidugli from the Biofuels lab at the Florida Institute of Technology for their valuable inputs on STL experiments and product characterization.

Appendix A. Supplementary data

Supplementary data to this article can be found online at https://doi.org/10.1016/j.ecmx.2021.100158.

References

[1] I. Tiseo. Breakdown of municipal waste materials generated in the U.S. 2018, by type; 2021.
[2] U.S.E.P. Agency. Advancing Sustainable Materials Management: Facts and Figures Report; 2018.
[3] Wang X, Jin Q, Zhang J, Li Y, Li S, Mikulčić H, et al. Soot formation during polyurethane (PU) plastic pyrolysis: The effects of temperature and volatile residence time. Energy Convers Manage 2018;164:353–62.
[4] Anuar Sharuddin SD, Abnisa F, Wan Daud WMA, Aroua MK. Energy recovery from pyrolysis of plastic waste: Study on non-recycled plastics (NRP) data as the real measure of plastic waste. Energy Convers Manage 2017;148:925–34.
[5] Wang J, Jiang J, Sun Y, Zhong Z, Wang X, Xia H, et al. Recycling benzene and ethylbenzene from in-situ catalytic fast pyrolysis of plastic wastes. Energy Convers Manage 2019;200:112088.
[6] Williams PT, Slaney E. Analysis of products from the pyrolysis and liquefaction of single plastics and waste plastic mixtures. Resour Conserv Recycl 2007;51(4):754–69.
[7] Qureshi MS, Oasmaa A, Pihkola H, Deviatkin I, Tenhunen A, Mannila J, et al. Pyrolysis of plastic waste: Opportunities and challenges. J Anal Appl Pyrol 2020;152:104804. https://doi.org/10.1016/j.jaap.2020.104804.
[8] Verma R, Vinoda KS, Papireddy M, Gowda ANS. Toxic Pollutants from Plastic Waste- A Review. Procedia Environ Sci 2016;35:701–8.
[9] Ma W, Chu C, Wang P, Guo Z, Liu B, Chen G. Characterization of tar evolution during DC thermal plasma steam gasification from biomass and plastic mixtures: Parametric optimization via response surface methodology. Energy Convers Manage 2020;225:113407. https://doi.org/10.1016/j.enconman.2020.113407.
[10] R. International. Environmental and Economic Analysis of Emerging Plastics Conversion Technologies; 2012.
[11] Maafa I. Pyrolysis of Polystyrene Waste: A Review. Polymers 2021;13(2):225. https://doi.org/10.3390/polym13020225.
[12] Font R, Fullana A, Caballero JA, Candela J, García A.. Pyrolysis study of polyurethane. J Anal Appl Pyrol 58-59; 2001: 63-77.
[13] Maric J, Berdugo Vilches T, Pissot S, Cañete Vela I, Gyllenhammar M, Seemann M. Emissions of dioxins and furans during steam gasification of Automotive Shredder residue; experiences from the Chalmers 2–4-MW indirect gasifier. Waste Manage 2020;102:114–21.
[14] Seshasayee Mahadevan Subramanya, Savage Phillip E. Oil from plastic via hydrothermal liquefaction: Production and characterization. Appl Energy 2020;278:115673. https://doi.org/10.1016/j.apenergy.2020.115673.
[15] Nakagawa T, Goto M. Recycling thermosetting polyester resin into functional polymer using subcritical water. Polym Degrad Stab 2015;115:16–23.
[16] Saha N, Saba A, McGaughy K, Reza MT. Effect of supercritical water temperature and Pd/C catalyst on upgrading fuel characteristics of gumweed-derived solvent-extracted biocrude. Biomass Convers Biorefin 2020.
[17] Reza MT, Coronella C, Holtman KM, Franqui-Villanueva D, Poulson SR. Hydrothermal Carbonization of Autoclaved Municipal Solid Waste Pulp and Anaerobically Treated Pulp Digestate. Acs Sustain Chem Eng. 2016;4:3649–58.
[18] Wilkes RA, Aristilde L. Degradation and metabolism of synthetic plastics and associated products by Pseudomonas sp.: capabilities and challenges. J Appl Microbiol 2017;123(3):582–93.
[19] Ghatge S, Yang Y, Ahn J-H, Hur H-G. Biodegradation of polyethylene: a brief review. Appl Biol Chem 2020;63:1–14.
[20] Oliveux G, Dandy LO, Leeke GA. Current status of recycling of fibre reinforced polymers: Review of technologies, reuse and resulting properties. Prog Mater Sci 2015;72:61–99.
[21] Saha N, Uddin MH, Reza MT. Preliminary safety evaluation of solvothermal liquefaction of plastic wastes using toluene as solvent. Clean Technol Environ Policy 2021;1–13.
[22] Shibasaki Y, Kamimori T, Kadokawa J-I, Hatano B, Tagaya H. Decomposition reactions of plastic model compounds in sub- and supercritical water. Polym Degrad Stab 2004;83:481–5.
[23] Damodharan D, Sathiyagnanam AP, Rana D, Rajesh Kumar B, Saravanan S. Extraction and characterization of waste plastic oil (WPO) with the effect of n-butanol addition on the performance and emissions of a DI diesel engine fueled with WPO/diesel blends. Energy Convers Manage 2017;131:117–26.
[24] Jie Huang, Ke Huang, Wenjie Qi, Zibin Zhu. Process analysis of depolymerization polybutylene terephthalate in supercritical methanol. Polym Degrad Stab 2006;91(10):2527–31.
[25] Mohsen-Nia M, Mohammad Doulabi FS. Separation of aromatic hydrocarbons (toluene or benzene) from aliphatic hydrocarbon (n-heptane) by extraction with ethylene carbonate. J Chem Thermodyn 2010;42:1281–5.
[26] Guo A, Wei Z, Zhao B, Chen K, Liu D, Wang Z, et al. Separation of Toluene-Insoluble Solids in the Slurry Oil from a Residual Fluidized Catalytic Cracking Unit: Determination of the Solid Content and Sequential Selective Separation of Solid Components. Energy Fuels 2014;28:3053–65.
[27] Brouwer T, Schuur B. Bio-based solvents as entrainers for extractive distillation in aromatic/aliphatic and olefin/paraffin separation. Green Chem 2020;22:5369–75.
[28] Hosokai Sou, Matsuoka Koichi, Kuramoto Koji, Suzuki Yoshizo. Modification of Dulong's formula to estimate heating value of gas, liquid and solid fuels. Fuel Process Technol 2016;152:399–405.
[29] Fulmer GR, Miller AJ, Sherden NH, Gottlieb HE, Nudelman A, Stoltz BM, et al. NMR chemical shifts of trace impurities: common laboratory solvents, organics, and gases in deuterated solvents relevant to the organometallic chemist. Organometallics 2010;29:2176–9.
[30] Cambridge Isotope Laboratories I. NMR Solvent Data Chart; 2010.
[31] Book C. Toluene(108-88-3) 1H NMR Related Products; 2017.
[32] Akiya N, Savage PE. Roles of water for chemical reactions in high-temperature water. Chem Rev 2002;102:2725–50.
[33] Zhao S, Wang C, Bai B, Jin H, Wei W. Study on the polystyrene plastic degradation in supercritical water/CO2 mixed environment and carbon fixation of polystyrene plastic in CO2 environment. J Hazard Mater 2022;421:126763.
[34] Huang J, Zeng G, Li X, Cheng X, Tong H. Theoretical studies on bond dissociation enthalpies for model compounds of typical plastic polymers. IOP Conference Series: Earth and Environmental Science. IOP Publishing; 2018. p. 012029.
[35] U.S.E.I. Administration. September 2021 Monthly Energy Review; 2021.
[36] Harano Y, Sato H, Hirata F. Solvent Effects on a Diels−Alder Reaction in Supercritical Water: RISM-SCF Study. J Am Chem Soc 2000;122:2289–93.
[37] Aljabri NM, Lai Z, Hadjichristidis N, Huang K-W. Renewable aromatics from the degradation of polystyrene under mild conditions. J Saudi Chem Soc 2017;21:983–9.
[38] Yu J, Biller P, Mamahkel A, Klemmer M, Becker J, Glasius M, et al. Catalytic hydrotreatment of bio-crude produced from the hydrothermal liquefaction of aspen

wood: a catalyst screening and parameter optimization study. Sustain Energy Fuels 2017;1:832–41.